

## Development of an active-detection mid-wave infrared search and track system based on "cat-eye effect"

ZHOU Pan-Wei<sup>1,2,3,4</sup>, DING Xue-Zhuan<sup>5,6\*</sup>, LI Fan-Ming<sup>2,3</sup>, YE Xi-Sheng<sup>1,2,4\*</sup>

1. Wangzhijiang Innovation Center for Laser, Shanghai Institute of Optics and Fine Mechanics, Chinese Academy of Sciences, Shanghai 201800, China;
2. Center of Materials Science and Optoelectronics Engineering, University of Chinese Academy of Sciences, Beijing 100049, China;
3. Shanghai Institute of Technical Physics, Chinese Academy of Sciences, Shanghai 200083, China;
4. Aerospace Laser Technology and System Department, Shanghai Institute of Optics and Fine Mechanics, Chinese Academy of Sciences, Shanghai 201800, China;
5. School of Instrument Science and Optoelectronic Engineering, Hefei University of Technology, Hefei 230009, China;
6. Weiyunpu (Suzhou) Optoelectronic Technology Co., Ltd, Suzhou 215400, China)

**Abstract:** In order to meet the urgent need of infrared search and track applications for accurate identification and positioning of infrared guidance aircraft, an active-detection mid-wave infrared search and track system (ADMWIRSTS) based on "cat-eye effect" was developed. The ADMWIRSTS mainly consists of both a light beam control subsystem and an infrared search and track subsystem. The light beam control subsystem uses an integrated opto-mechanical two-dimensional pointing mirror to realize the control function of the azimuth and pitch directions of the system, which can cover the whole airspace range of  $360^{\circ} \times 90^{\circ}$ . The infrared search and track subsystem uses two mid-wave infrared cooled  $640 \times 512$  focal plane detectors for co-aperture beam expanding, infrared and illumination laser beam combining, infrared search, and two-stage track opto-mechanical design. In this work, the system integration design and structural finite-element analysis were conducted, the search imaging and two-stage track imaging for external scenes were performed, and the active-detection technologies were experimentally verified in the laboratory. The experimental investigation results show that the system can realize the infrared search and track imaging, and the accurate identification and positioning of the mid-wave infrared guidance, or infrared detection system through the echo of the illumination laser. The aforementioned work has important technical significance and practical application value for the development of compactly-integrated high-precision infrared search and track, and laser suppression system, and has broad application prospects in the protection of equipment, assets and infrastructures.

**Key words:** active-detection, mid-wave infrared search and track, "cat-eye effect", illumination laser, light beam control

## 基于“猫眼效应”的主动探测中波红外搜跟系统研制

周潘伟<sup>1,2,3,4</sup>, 丁学专<sup>5,6\*</sup>, 李范鸣<sup>2,3</sup>, 叶锡生<sup>1,2,4\*</sup>

1. 中国科学院上海光学精密机械研究所 王之江激光创新中心, 上海 201800;
2. 中国科学院大学 材料与光电研究中心, 北京 100049;
3. 中国科学院上海技术物理研究所, 上海 200083;
4. 中国科学院上海光学精密机械研究所 空天激光技术与系统部, 上海 201800;

Received date: 2024-11-22, revised date: 2025-02-24

收稿日期: 2024-11-22, 修回日期: 2025-02-24

Foundation items: Supported by the Fundamental Scientific Research Plan of China (JCKY2021130B033)

Biography: ZHOU Pan-Wei (1985-), male, Jiangxi, associate research fellow, Ph. D. candidate. Research area involves infrared optical mechanical integration, infrared search and track, and laser integration. E-mail: zp-wei@163.com

\*Corresponding authors: E-mail: xsye@siom. ac. cn, dingxuezhuan@163.com

5. 合肥工业大学 仪器科学与光电工程学院, 安徽 合肥 230009;  
6. 微云谱(苏州)光电科技有限公司, 江苏 苏州 215400)

**摘要:** 为了满足红外搜索跟踪应用对于红外导引装置进行精确识别与定位的迫切需求, 本文进行了一种基于“猫眼效应”的主动探测中波红外搜跟系统(ADMWIRSTS)研制, 该系统主要由光束控制分系统和红外搜跟分系统组成。光束控制分系统采用光机一体二维指向镜实现系统方位、俯仰方向控制功能, 可覆盖 $360^\circ \times 90^\circ$ 全空域范围。红外搜跟分系统采用两个中波红外制冷式 $640 \times 512$ 焦平面探测器进行了共孔径扩束、红外与照明激光合束、红外搜索、两级跟踪光机设计。本工作中, 进行了系统集成设计及结构有限元分析, 对外场景物进行了搜索成像及两级跟踪成像, 并在实验室对主动探测技术进行了实验验证。实验结果显示, ADMWIRSTS可通过照明激光的回波实现对中波红外导引或红外探测系统进行红外搜索跟踪成像及精确识别定位。上述工作对于发展紧凑型高精度红外搜跟与激光压制一体化系统等具有重要的技术意义和实际应用价值, 在装备、物资和基础设施防护方面有广阔的应用前景。

**关键词:** 主动探测; 中波红外搜跟; “猫眼效应”; 照明激光; 光束控制

中图分类号: TN216

文献标识码: A

## Introduction

With the continuous progress of infrared imaging technology, its threat to high-value targets is also growing, and its prominent role is in the application of infrared guided aircraft. In the Gulf of 1991, the US, with a huge scientific and technological advantage, lost only 19 aircraft, most of which were shot down due to the role of infrared guidance<sup>[1]</sup>. Under the traction needs, infrared imaging guidance technology has become a hot spot in the development of photoelectric precision guidance technology<sup>[2]</sup>. Especially after the Gulf of 1991, the various kinds of aircrafts relying on infrared imaging technology have been successfully used, making infrared guidance technology become the focus of research on high-value target strike technology<sup>[3,4]</sup>. To cope with the threat of infrared guidance system to high-value targets, the technical demand for rapid and effective protection of high-value facilities or equipment during photoelectric guidance or optical imaging moving targets approach is increasing. The infrared guidance system can be simplified into two parts: infrared optical lens and infrared detector. The infrared detector is the core component that converts thermal radiation into electrical signals. Direct interference or damage to the infrared detector can cause the infrared guidance system to fail. Laser is called "the fastest knife", "the most accurate ruler" and "the brightest light", which is the best means to interfere with or damage the infrared detector. However, how to accurately identify and locate the infrared guidance system during search and track is a big challenge.

The infrared search and track (IRST) system is a device that uses the principle of infrared imaging to accurately search and track targets. As a passive detection method, infrared search and track has the advantages of strong anti-interference ability, good concealment and all-weather work<sup>[5-7]</sup>. In the infrared band, the 3-5  $\mu\text{m}$  of the mid-infrared band is in the atmospheric window, and the transmittance in the atmosphere is high<sup>[8]</sup>. Moreover, the tail flame spectrum formed by fuel combustion of important targets such as aircrafts, powered missiles and rockets is also mostly in the mid-infrared band of 3-5  $\mu\text{m}$ <sup>[9]</sup>.

Therefore, the 3-5  $\mu\text{m}$  mid-wave infrared band occupies a very important position in infrared guidance systems, infrared lasers, and infrared search and track.

The OEPS-29 infrared search and track system, equipped by Russia's Su-27 SK, uses a 64-element linear indium antimonide infrared detector. The infrared azimuth instrument, laser range finder and helmet targeting device are integrated together to form an application system. The scanning range is: azimuth  $-60^\circ - 60^\circ$ , pitch  $-15^\circ - 60^\circ$ , and the system mass is 175 kg<sup>[10]</sup>. The Dutch "Sirius" is the most typical linear array scanning infrared search and tracking system in the early days. The system includes two cooled infrared detectors, which work in the 3-5  $\mu\text{m}$  mid-wave infrared and 8-12  $\mu\text{m}$  long-wave infrared bands respectively. The resolutions of the two detectors are  $300 \times 10$  and  $300 \times 8$ , respectively<sup>[11]</sup>. SIMONE, an infrared surveillance, observation, and navigation system developed by Germany's Diehl BGT Defense Company, has a  $360^\circ$  search capability. The first SIMONE system was put into service on the German Navy's new F125 frigate in 2017. The SIMONE system uses multiple detector stare imaging, with each detector module using a  $640 \times 512$  uncooled detector operating in the 8-12  $\mu\text{m}$  band, with a single detector module having an azimuth coverage of  $40^\circ$  and an elevation range of  $50^\circ$ <sup>[12]</sup>. The Dutch IRSCAN infrared search and track system is designed for destroyers, with a scanner head weighing about 75 kg, a pitch field view of  $14.6^\circ$ , an azimuth coverage of  $360^\circ$ , and uses a 1024-element focal plane array detector operating in the 8-14  $\mu\text{m}$  band<sup>[13]</sup>.

According to the results of the literature survey, domestic research on the application of infrared search and track system started late and there are few publicly available related materials. The advanced technology countries have carried out extensive research on infrared search and track system, but there is no compact optomechanical integrated system design with two-stage track and infrared illumination laser integration, and it is impossible to accurately identify and locate the infrared guidance system by active detection, which cannot meet the effective application requirements for infrared guidance system. Moreover, there are few public research re-

sults in this area. This paper innovatively realizes the engineering application of the active-detection mid-wave infrared search and track system (ADMWIRSTS) based on "cat-eye effect", and completes the integration of infrared search, two-stage infrared track, mid-wave laser illumination and light beam control functions using two mid-wave infrared cooled  $640 \times 512$  focal plane detectors for detection. The echo of the illumination laser is received by the fine track module, and the integrated application of infrared search and track, and illumination laser is finally realized. The ADMWIRSTS is designed with compact opto-mechanical integration. The size of the ADMWIRSTS is 660 mm (length)  $\times$  607 mm (width)  $\times$  664 mm (height), and the mass is less than 68 kg, which meets the requirements of compact and lightweight engineering application. The ADMWIRSTS developed in this paper carries out the co-aperture transmission and reception of infrared search and track, and mid-wave illumination laser, and searches for targets in the 3-5  $\mu\text{m}$  band, and then locks onto targets with coarse and fine track. It can accurately identify and locate the infrared guidance or infrared detection system through the echo of the illumination laser, with an infrared identification resolution better than 35  $\mu\text{rad}$ . The results of outfield imaging and laboratory experiments show that the system can realize the accurate identification and positioning of active detection in infrared search and tracking imaging for mid-wave infrared guidance or infrared detection system, and the engineering application effect is good.

## 1 System principle

In optical systems, there is a physical property known as "cat-eye effect". When the cat's eyes are irradiated with light in the night, bright light will be emitted. This is because the cat's retina has a very high reflectivity of light. When the light passes through the pupil and enters the retina, it can return in the same way. This is so-called "cat-eye effect"<sup>[14]</sup>. In the optical imaging system, the "cat-eye effect" can be simplified as the model shown in Fig. 1, which is composed of the converging lens and the focal plane. When the beam EF parallel to the optical axis of the lens converges to the focal plane through the lens, it can be known from the reversibility of the light that the reflected beam will return along the FE direction. Similarly, when the obliquely incident beam MN converges to the focal plane through the lens, the reflected beam will return along the NM direction<sup>[15-16]</sup>. For laser irradiation, the "cat-eye effect" reflection light, due to the focusing reflection of the lens, will have an echo light energy higher than that of ordinary target echoes<sup>[17-19]</sup>.

The application of the laser "cat-eye effect" in foreign optoelectronic systems started earlier, and has formed a variety of engineering applications such as vehicle-mounted active laser systems, anti-sniper laser systems, ship-mounted and airborne active laser systems<sup>[20-22]</sup>. However, there are few publicly available engineering application results of the mid-infrared "cat-eye effect" both domestically and internationally.

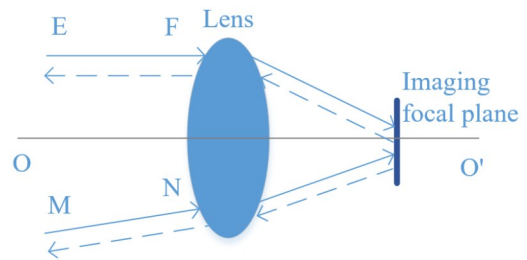


Fig. 1 The schematic diagram of "cat-eye effect"  
图1 "猫眼效应"示意图

The technical route of the ADMWIRSTS based on "cat-eye effect" is that the mid-wave infrared search and track identifies the target through infrared search, and locks the target through coarse track and fine track. After emitting laser with the illumination laser of the common optical path of fine track, the target is accurately identified and located through the active detection of the "cat-eye effect".

As shown in Fig. 2, the ADMWIRSTS mainly includes a light beam control subsystem and an infrared search and track subsystem. The main body of the light beam control subsystem adopts a high-precision two-dimensional pointing mechanism, which realizes the light beam control function through the movement of the path turning and the opto-mechanical reflecting mirror. The opto-mechanical two-dimensional motion mechanism can cover the whole airspace range of  $360^\circ \times 90^\circ$ .

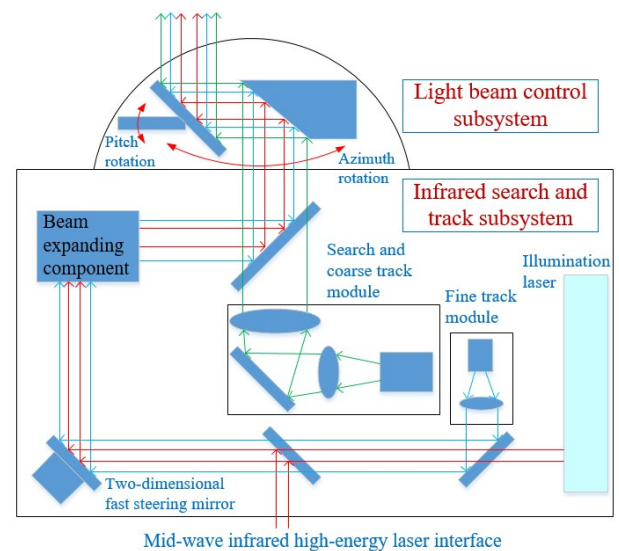


Fig. 2 Principle block diagram of active-detection mid-wave infrared search and track system (ADMWIRSTS)  
图2 主动探测中波红外搜跟系统原理框图

The infrared search and track subsystem mainly includes search and coarse track module, fine track module, two-dimensional fast steering mirror, beam expanding component and illumination laser.

The mirror of the light beam control subsystem rotates continuously in the azimuth direction in the search mode, and the infrared search and coarse track module

searches and images the  $360^\circ$  scene in the azimuth direction. In the azimuth continuous search, the pitch drive mechanism adjusts the pitch angle (pitch baseline) of the visual axis center of the imaging field to complete the whole airspace search. In the track mode, the main function of the infrared search and coarse track module is to receive the thermal radiation of the target, and use target-missing quantity information of the target to drive the two-dimensional opto-mechanical scanning mechanism of the light beam control subsystem to realize the passive coarse track of the target.

The main function of the fine track module is to actively detect the target echo under the illumination of the laser, accurately identify and locate the target optical system according to the principle of "cat-eye effect", extract the target-missing quantity of the target, drive the two-dimensional fast steering mirror to accurately correct the target optical axis at the  $\mu\text{rad}$  level, and realize the further accurate track function of the target optical system.

The system's search and coarse track function is completed by combining search and coarse track with light beam control. The combination of coarse track and fine track is used to accurately identify and locate the target optical system. The system completes the integrated design of infrared search, infrared track and light beam control functions, and finally realizes the integrated application of infrared search and track, and illumination laser.

The opto-mechanical interface of the mid-wave infrared high-energy laser is reserved in the active detection system. In the coarse track, the light beam control subsystem locks the target. After the fine track accurately identifies and locates the target optical system, the high-energy laser can be emitted in the fine track optical path for laser damage irradiation.

## 2 Light beam control subsystem design

### 2.1 Light beam control subsystem opto-mechanical design

The schematic diagram of the principle of the light beam control subsystem is shown in Fig. 3. The main body of the light beam control subsystem adopts an opto-mechanical miniaturized two-dimensional pointing mechanism. Through the optical path turning and the movement of the opto-mechanical mirror, the infrared search and track optical path and the laser beam are controlled in the azimuth and pitch directions. The opto-mechanical two-dimensional pointing and scanning motion mechanism includes azimuth mechanism and pitch mechanism, which can cover the whole airspace range of  $360^\circ \times 90^\circ$ . The light beam control subsystem is mainly composed of azimuth drive mechanism, pitch drive mechanism, turning mirror and scanning mirror. The turning mirror and scanning mirror rotate around the azimuth axis, and the scanning mirror rotates around the pitch axis to realize the field of view of the system covering the airspace.

The opto-mechanical structure of the light beam control subsystem is shown in Fig. 4. The main body is a compact and lightweight two-dimensional turntable that

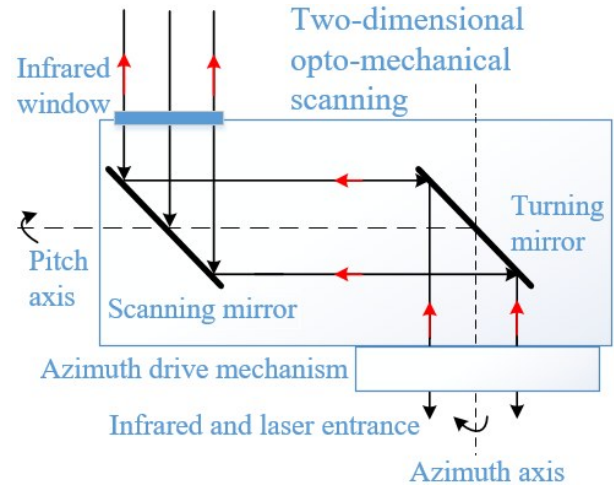


Fig. 3 Principle diagram of light beam control subsystem  
图3 光束控制分系统原理示意图

drives the azimuth and pitch rotation of the scanning mirror. The overall size is  $460 \text{ mm}$  (diameter)  $\times$   $362 \text{ mm}$  (height). The weight of the subsystem is about  $20 \text{ kg}$ , which meets the use demand of miniaturized system. The pitch scanning mirror is a reflector mirror installed at a  $45^\circ$  angle, and the pitch driving mechanism drives the pitch scanning mirror to pitch rotate around the rotation center. Through the optical reflection of the pitch-rotating pitch scanning mirror and the fixed  $45^\circ$  reflector, the search and track optical path and the laser beam rotate in the pitch  $90^\circ$  range, and the azimuth rotation is driven by the azimuth drive mechanism, so as to search and track imaging in the airspace. The pitch scanning mirror and  $45^\circ$  reflector are designed by opto-mechanical integration. The material is 7075-T6 high-performance aviation aluminum alloy, and the diameter of the reflected optical path is  $84 \text{ mm}$ . The sealed upper ball cover of the azimuth rotation part adopts an approximate hemispherical design, which greatly reduces the wind resistance during azimuth rotation. The light-transmitting hole of the light beam control subsystem is  $86 \text{ mm}$ .

The pitch drive mechanism, the pitch scanning mirror and the  $45^\circ$  reflector are installed on the scanning base slab. The upper ball cover seals the reflector, search and track optical path and laser beam are emitted from the infrared window. The azimuth drive mechanism is installed on the outer cover supporting pedestal to drive the scanning base slab to rotate  $360^\circ$  in azimuth, completing the azimuth rotation of the pitch scanning mirror and the  $45^\circ$  reflector around the azimuth axis. Hollow electric slip ring is installed between the rotating end and the fixed end of the azimuth rotation to meet the electronic interface connection during continuous rotation. At the same time, the center of the azimuth drive mechanism is a hollow light hole structure for optical path and beam transmission.

### 2.2 Calculation of light beam control motion parameters

In order to ensure the reliability of the spatial pointing of the light beam control subsystem, the motion pa-

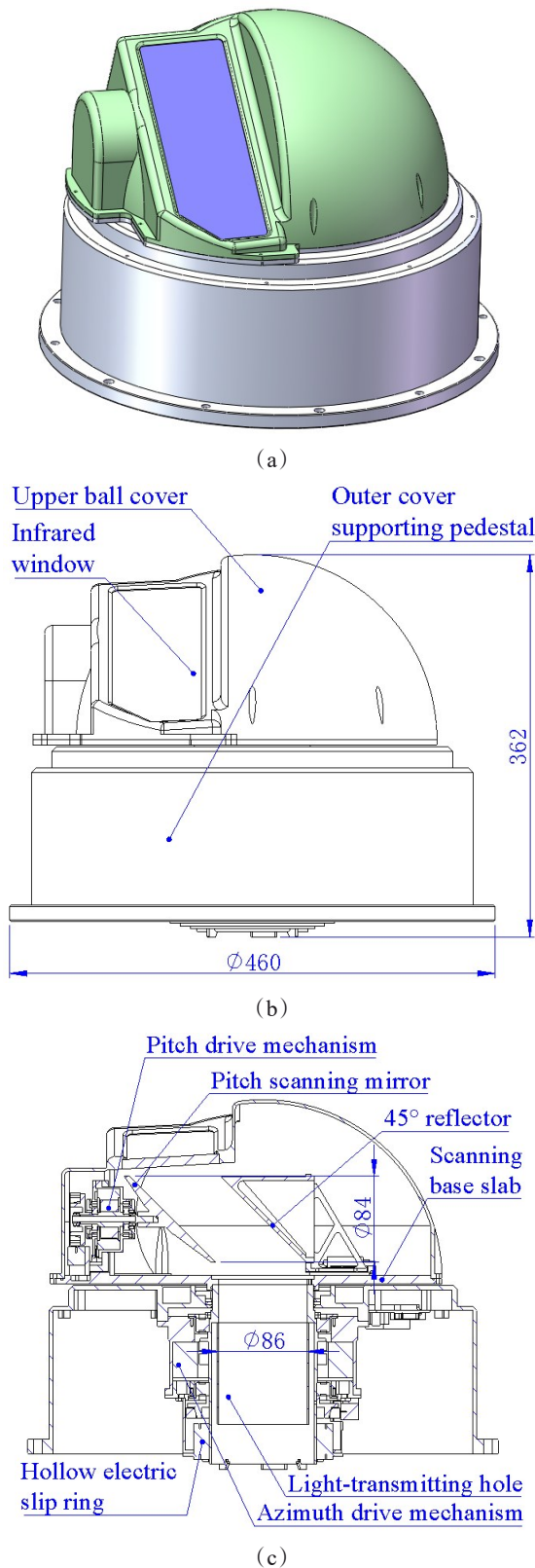


Fig. 4 Opto-mechanical structure of light beam control subsystem: (a) 3D model; (b) front view; (c) section view  
图4 光束控制分系统光机结构:(a)三维模型;(b)前视图;(c)剖视图

parameters of the two-dimensional pointing mechanism are analyzed and calculated. According to the system re-

quirements, the time  $t$  pointing to the rotation is 1 s, and the rotation angle is  $90^\circ$  within 1 s in the pitch direction. Because the azimuth direction can be rotated in the forward or reverse direction, the rotation angle is  $180^\circ$  within 1 s in the azimuth direction. The two-stage control strategy of "equal acceleration + equal deceleration" is adopted in the rotation process. The relationship between the rotation time  $t$  and the speed  $v$  is shown in Fig. 5,  $a$  is the angular acceleration, and  $at/2$  is the maximum angular velocity in the rotation process.

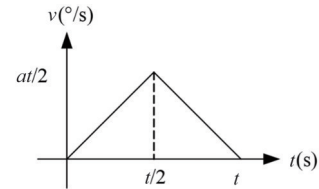


Fig. 5 The relationship between rotation time and speed  
图5 调转时间和转速的关系

According to the relationship between the rotation time and the speed, the calculation Eq. (1) of the rotation stroke can be obtained:

$$S = \frac{at^2}{4} \quad (1)$$

In Eq. (1),  $S$  is the angle stroke of the scanning pitch mirror in the pitch or azimuth direction of the system in 1 s, with pitch stroke  $S_p=90^\circ$ , azimuth stroke  $S_a=180^\circ$ ,  $t=1$  s. Through Eq. (1) and the relationship between rotation time and speed, the pitch angular acceleration  $a_p$ , the pitch maximum angular velocity  $v_p$ , the azimuth angular acceleration  $a_a$ , and the azimuth maximum angular velocity  $v_a$  can be obtained, as shown in Table 1, rpm (Revolutions Per Minute) represents the number of circumferential rotations per minute of the motor.

Table 1 System pitch and azimuth angular acceleration, maximum angular velocity  
表1 系统俯仰及方位的角加速度、最大角速度

Parameter	Index
Pitch angular acceleration $a_p$	$360^\circ/s^2$
Pitch maximum angular velocity $v_p$	$180^\circ/s$ (30 rpm)
Azimuth angular acceleration $a_a$	$720^\circ/s^2$
Azimuth maximum angular velocity $v_a$	$360^\circ/s$ (60 rpm)

As shown in Table 1, the maximum theoretical speed of the pitch drive mechanism should not be less than 30 rpm, and the maximum theoretical speed of the azimuth drive mechanism should not be less than 60 rpm.

The pitch rotation load of the light beam control subsystem mainly includes the pitch scanning mirror, the pitch grating encoder, the pitch shaft system rotation part and the pitch torque motor rotation part. The azimuth rotation load mainly includes the upper ball cover, the pitch drive mechanism, the pitch scanning mirror, the  $45^\circ$  reflector, the scanning base slab, the azimuth grating encoder, the azimuth shaft system rotation part, the

azimuth torque motor rotation part. The mass of the load and the moment of inertia around the rotation axis are obtained from the three-dimensional design model. The light beam control subsystem servo load parameter indices are shown in Table 2.

**Table 2 Servo load parameter indices of light beam control subsystem**

表2 光束控制分系统伺服负载参数指标

Parameter	Index
Pitch load mass $m_p$	0.44 kg
Pitch moment of inertia $J_p$	$1.53 \times 10^{-4} \text{ kg} \cdot \text{m}^2$
Azimuth load mass $m_a$	8.65 kg
Azimuth moment of inertia $J_a$	$0.13 \text{ kg} \cdot \text{m}^2$

The continuous torque  $T_{rms}$  of the drive motor is determined by Eq. (2):

$$T_{rms} = \sqrt{\frac{T_a^2 \times t_a + T_f^2 \times t_z + T_b^2 \times t_b}{t}} \quad (2)$$

In Eq. (2):

$$T_f = \frac{d\mu m a_h}{2\eta} \quad (3)$$

$$T_a = \frac{3.14 \times J a}{180} T_f \quad (4)$$

$$T_b = \frac{3.14 \times J a}{180} - T_f \quad (5)$$

In Eqs. (2) - (5),  $T_f$  is the friction torque that needs to be overcome in the rotation,  $d$  is the inner diameter of the bearing,  $d_p=10$  mm in the pitch drive mechanism,  $d_a=110$  mm in the azimuth drive mechanism,  $\mu$  is the friction coefficient,  $\mu$  is 0.1,  $m$  is the load mass,  $a_h$  is the sum of the vibration acceleration and the gravity acceleration in the vertical horizontal direction,  $a_h=2.5 \text{ g}=24.5 \text{ m/s}^2$ ,  $\eta$  is the efficiency,  $\eta$  is 0.8;  $T_a$  is the torque required for the acceleration section in the system rotation, and  $T_a$  is the maximum peak torque required for the mechanism;  $T_b$  is the torque required for the deceleration section of the system,  $J$  is the moment of inertia of the load around the rotation axis, and  $a$  is the angular acceleration;  $t_a$  is the acceleration time in the rotation,  $t_a=0.5$  s,  $t_z$  is the uniform speed time in the rotation,  $t_z=0$  s,  $t_b$  is the deceleration time in the rotation,  $t_b=0.5$  s,  $t$  is the total rotation time of the system,  $t=1$  s.

From Tables 1 and 2, the angular acceleration, load mass and moment of inertia in pitch and azimuth rotation can be obtained. Through Eqs. (2) - (5), the continuous torque and peak torque required by the pitch drive mechanism and the azimuth drive mechanism can be obtained, as shown in Table 3. The calculation result of  $T_{bp}$  is negative, indicating that the pitch drive motor has the same torque action direction in the acceleration section and the deceleration section, and the pitch rotation ability can reach a higher level under this torque.

**Table 3 Continuous torque and peak torque of pitch and azimuth drive mechanism**

表3 俯仰及方位驱动机构的连续转矩、峰值转矩

Parameter	Index
Pitch drive mechanism continuous torque $T_{mcp}$	$0.7 \times 10^{-2} \text{ N} \cdot \text{m}$
Pitch drive mechanism peak torque $T_{ap}$	$0.8 \times 10^{-2} \text{ N} \cdot \text{m}$
Azimuth drive mechanism continuous torque $T_{msa}$	$2.2 \text{ N} \cdot \text{m}$
Azimuth drive mechanism peak torque $T_{sa}$	$3.1 \text{ N} \cdot \text{m}$

### 3 Infrared search and track subsystem design

#### 3.1 Infrared search and track subsystem overall design

The overall design of the infrared search and track subsystem is shown in Fig. 6, which mainly includes the search and coarse track module, fine track module, beam expanding component, two-dimensional fast steering mirror, and illuminating laser, with dimensions of 660 mm (length)  $\times$  562 mm (width)  $\times$  332 mm (height), and the weight of the subsystem is about 42 kg. All components of the infrared search and track subsystem are installed on the search and track integrated base slab, which has good structural stiffness while being lightweight. The infrared search and track subsystem uses sealed outer cover to seal the subsystem, and electronic interfaces are designed on the cover for power and image transmission, and communication connections.

The two-dimensional fast steering mirror and illumination laser technology in the infrared search and track subsystem are relatively mature, and the mature scientific research supporting equipment on the market is adopted. The size of the two-dimensional fast steering mirror is 112 mm (length)  $\times$  71 mm (width)  $\times$  93.5 mm (height), the weight is about 1 kg, the two-dimensional rotation stroke is  $\pm 20$  mrad, the accuracy is about 5  $\mu$ rad, and the optical aperture is 70 mm. The size of the illumination laser is 315 mm (length)  $\times$  166 mm (width)  $\times$  97 mm (height), the weight is about 6 kg, the laser output wavelength is 3.7  $\mu$ m, the repetition rate is not less than 9 kHz, the average power is about 3 W, the divergence angle is 5 mrad, and the beam diameter is 6 mm.

#### 3.2 Beam expanding component and opto-mechanical beam combination

In the infrared search and track subsystem, the fine track optical path and the illumination laser beam are co-aperture beams expanded through the beam expanding component. The beam expanding component adopts reflective optical beam expanding, and its functions mainly include: 1) increasing the spot diameter of the illumination laser; 2) reduce the divergence angle of the laser beam; 3) as the main receiving mirror of the fine track detection, receiving the illumination laser "cat-eye effect" echo, to achieve accurate identification and positioning of the target by laser active detection. The optical design parameter indices of the beam expanding component are shown in Table 4, and the optical path diagram

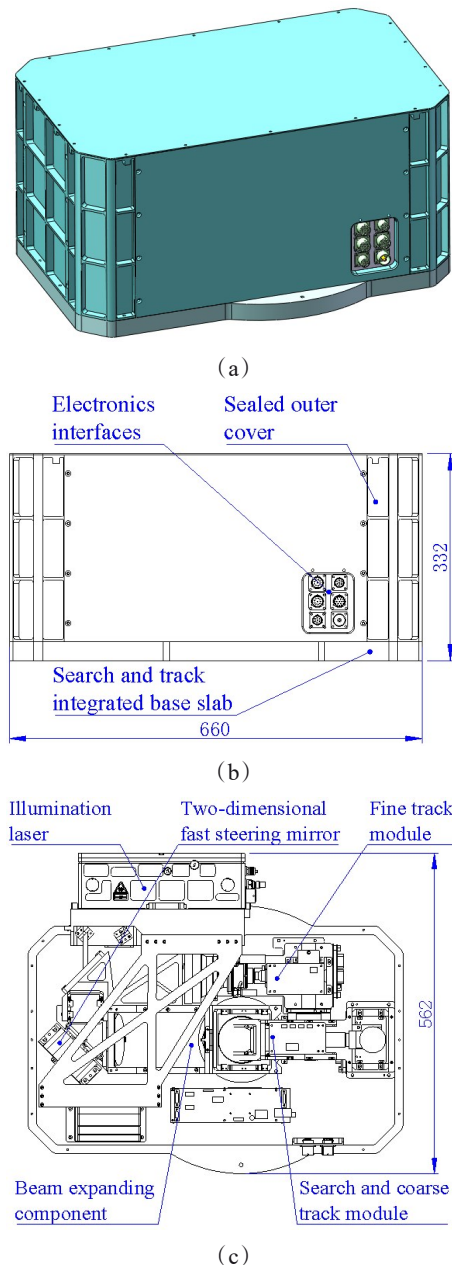


Fig. 6 Overall design of infrared search and track subsystem: (a) 3D model; (b) front view; (c) upper view (the sealed outer cover is hidden)

图6 红外搜跟分系统总体设计:(a)三维模型;(b)前视图;(c)上视图(隐藏密封外罩)

is shown in Fig. 7.

The schematic diagram of the search and track opto-

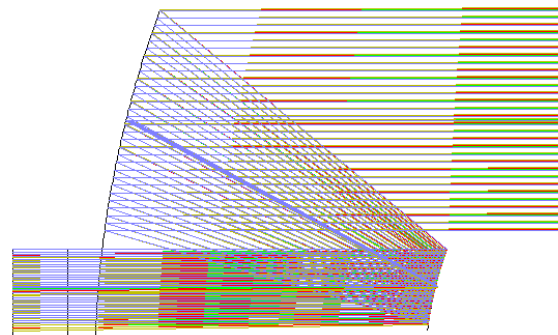


Fig. 7 Beam expanding component optical path diagram  
图7 扩束组件光路图

mechanical beam combining is shown in Fig. 8. The dotted line in the figure represents the fine track optical path. The fine track optical path and the illumination laser beam pass through the beam combining mirror 1 to perform the opto-mechanical integrated beam combining of infrared and illumination laser; the beam combining mirror 2 is a reserved beam combining mirror, which can perform co-aperture beam combining of mid-wave infrared high-energy laser beams in the fine track optical path, and its function is to reserve a high-energy laser interface; the fine track optical path and the search and coarse track optical path are opto-mechanical integration beam combining of the infrared search and track through the beam combining mirror 3. The infrared optical path is combined with the laser beam to form a co-aperture outgoing optical path.

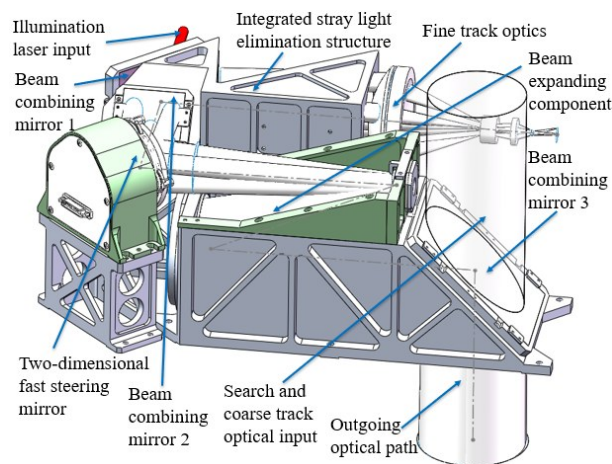


Fig. 8 Search and track opto-mechanical beam combining schematic diagram

图8 搜跟光机合束示意图

From Fig. 8, the fine track optics is at the front position of the search and track opto-mechanical beam combining optical path, and the search and coarse track optics is at the end position of the search and track opto-mechanical beam combining optical path. The fine track optical path and the illumination laser beam share the same optical path in the whole search and track optical path. The fine track pointing is performed by the two-dimen-

Table 4 Optical design parameter indices of beam expanding component

Parameter	Index
Beam expanding band	Mid-wave infrared
Beam expanding ratio	5
Reflectance	98%
Anti-laser damage threshold	30 MW/cm <sup>2</sup>

表4 扩束组件光学设计参数指标

sional fast steering mirror, and the optical path is expanded by 5 times by the beam expanding component. After beam expansion, the illumination laser divergence angle is 1 mrad, and the beam diameter is 30 mm. An integrated stray light elimination structure is designed between the beam combing 1 and the fine track optics to eliminate and absorb the stray light.

### 3.3 Search and coarse track module design

The detector of the search and coarse track module uses an area array cooled infrared detector. The imaging output frame frequency is not less than 100 Hz, and the effective aperture is 55 mm. The optical design parameters of the search and coarse track module are shown in Table 5.

**Table 5 Search and coarse track optical parameters**  
表5 搜索及粗跟踪光学参数

Parameter	Index
Band range	3.7–4.8 $\mu\text{m}$
Detector pixel number	640×512
Detector pixel size	15 $\mu\text{m}$ ×15 $\mu\text{m}$
F number	2
Imaging field angle	5°×4°
Focal length	110 mm

Search and coarse track optical lens is designed to achieve a compact structural layout, using a secondary imaging with a total of 6 lenses and a reflector in the middle for optical path turning. The opto-mechanical structure of the search and coarse track module is shown in Fig. 9. The detector and lens of the search and coarse track module are installed on the search and coarse track base slab. To make the system structure compact, the lens makes a 90° turning of the optical path, and the bottom of the module is supported by two support frames.

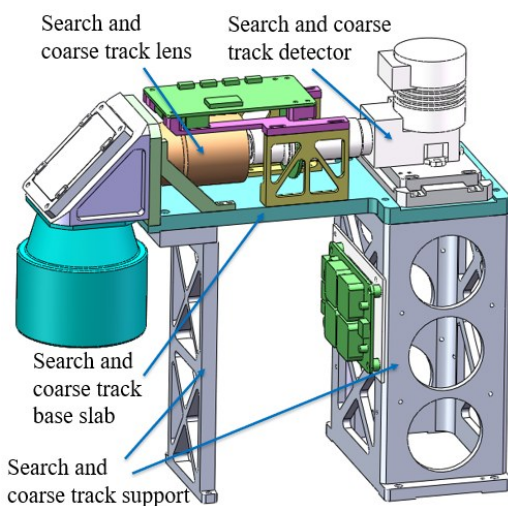


Fig. 9 Opto-mechanical structure of search and coarse track module

图9 搜索及粗跟踪模块光机结构

The optical path of the search and coarse track module is shown in Fig. 10.

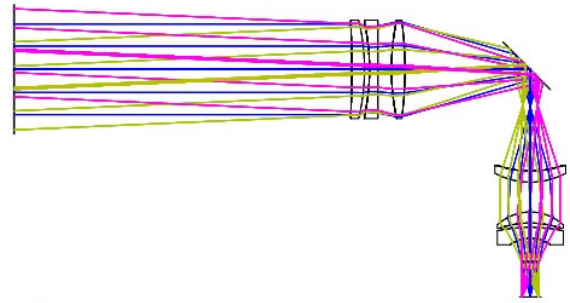


Fig. 10 Search and coarse track module optical path diagram  
图10 搜索及粗跟踪模块光路图

The single-pixel instantaneous field of view of the search and coarse track module is 0.136 mrad, and the athermalization design is adopted. According to the MTF (Modulation Transfer Function) curves of the athermalization design of the search and coarse track module at different temperatures in Fig. 11, the athermalization design of the search and coarse track module is good, which can ensure the imaging quality of the search and coarse track module in high and low temperatures.

### 3.4 Fine track module design

The detector of the fine track module uses an area array cooled infrared detector. The imaging output frame frequency is not less than 100 Hz, and the effective aperture is 80 mm. The optical design parameters of the fine track module are shown in Table 6.

The optical lens design of the fine track module uses 4 lenses for one imaging design. The opto-mechanical structure of the fine track module is shown in Fig. 12. The detector and lens of the fine track module are installed on the fine track base slab. A cam-type focusing mechanism is used to compensate for the focal length changes of the fine tracking module in high and low temperatures. The bottom of the module is supported by two support frames.

The fine track module passes through the beam expanding component and beam combining mirror, two-dimensional fast steering mirror optical path turning, and the optical path diagram is shown in Fig. 13.

The single-pixel instantaneous field of view of the fine track module is 34.1  $\mu\text{rad}$ , and the temperature focusing compensation design is adopted. It can be seen from the MTF curve of the fine track module in Fig. 14 that the theoretical limit MTF of the 33 lp(line-pairs)/mm in Fig. 14(a) is low due to the high  $F$  number in the fine track optical design. On the basis of maintaining the same resolution as the search and coarse track, the MTF of the 17 lp/mm is analyzed as shown in Fig. 14(b). It can be seen from Fig. 14 that the optical design of the fine track module is good, which can ensure the imaging quality.



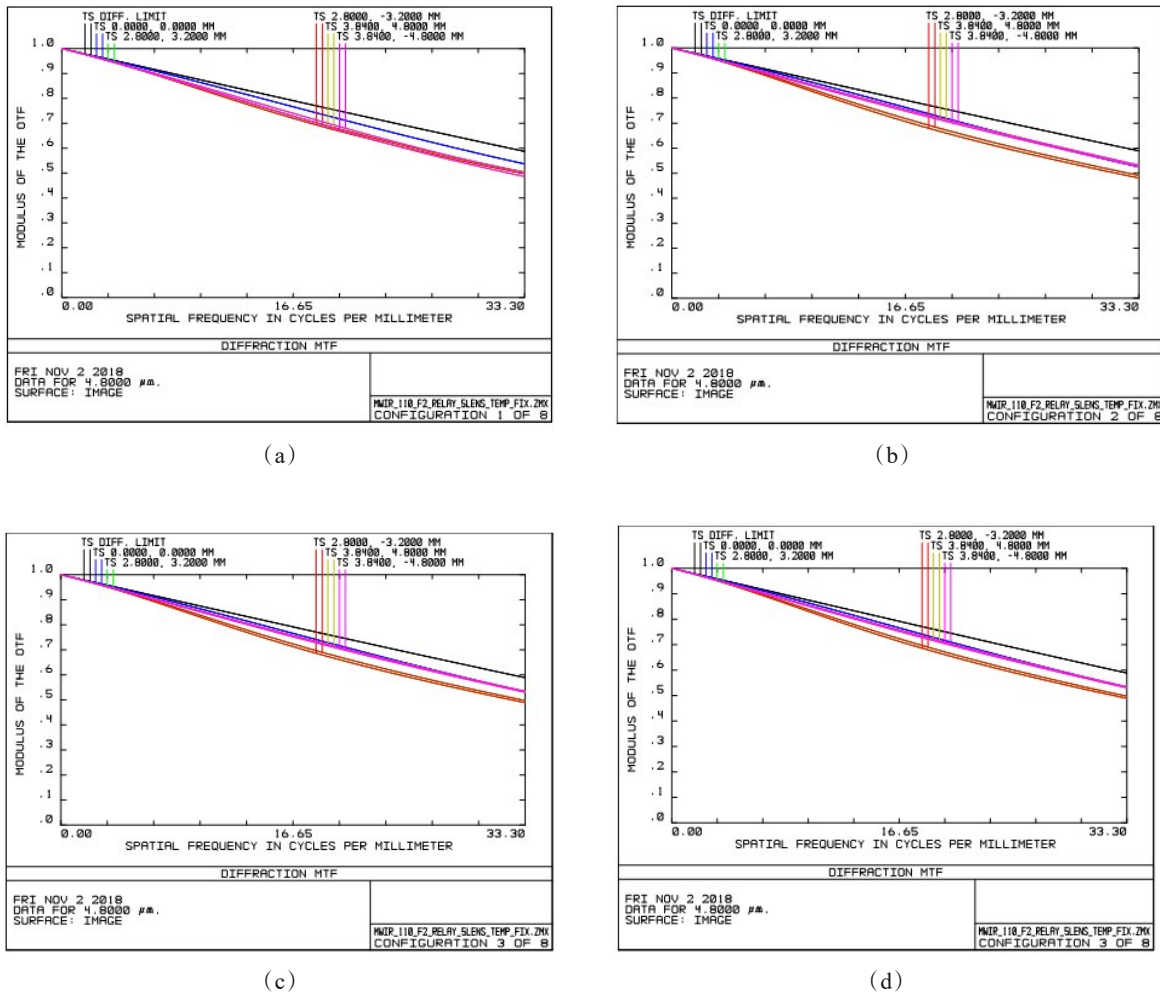


Fig. 11 Search and coarse track module athermalization design MTF at different temperatures: (a) 20 °C; (b) -55 °C; (c) 0 °C; (d) 70 °C  
 图 11 搜索及粗跟踪模块无热化设计不同温度 MTF: (a)20 °C; (b)-55 °C; (c)0 °C; (d)70 °C

Table 6 Fine track optical parameters  
 表 6 精跟踪光学参数

Parameter	Index
Band range	3.7-4.8 μm
Detector pixel number	640×512
Detector pixel size	15 μm×15 μm
F number	5.5
Imaging field angle	1.25°×1°
Focal length	440 mm

## 4 System integration and experimental verification

### 4.1 System integration and simulation

The integrated design of the ADMWIRSTS is shown in Fig. 15. The infrared search and track subsystem adopts an inverted structure, and the light beam control subsystem is installed on the search and track integrated base slab of the infrared search and track subsystem for

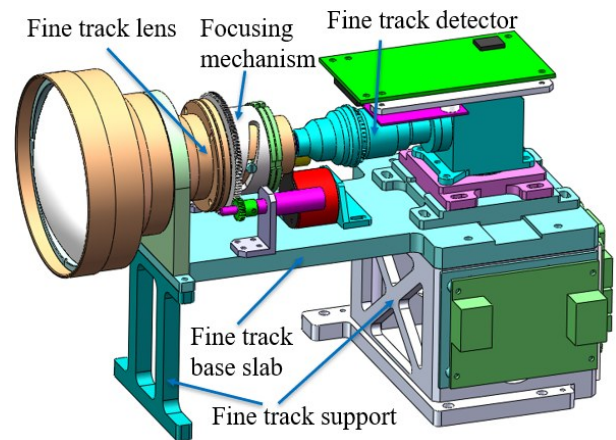


Fig. 12 Opto-mechanical structure of fine track module  
 图 12 精跟踪模块光机结构

system integration. The search and track support plate is installed on the outer ring of the active detection system

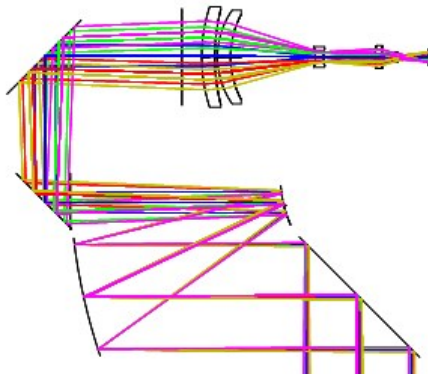
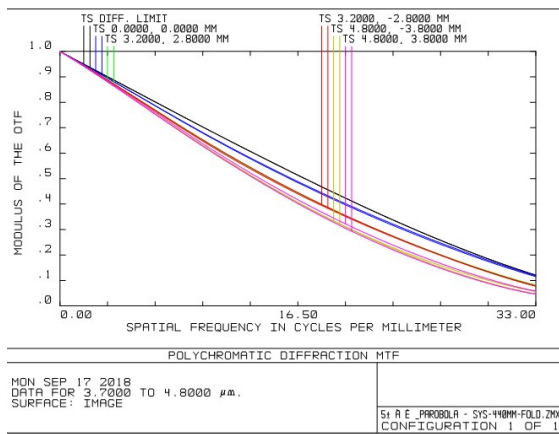
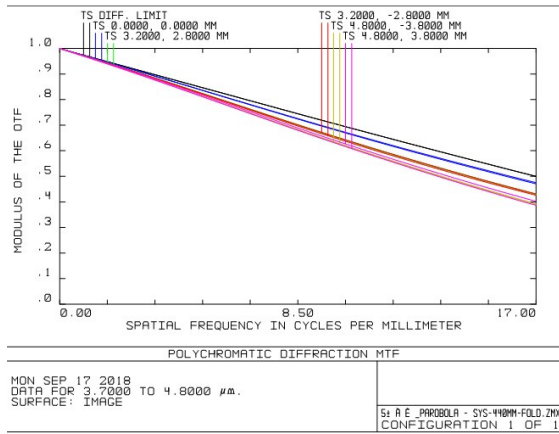


Fig. 13 Fine track module optical path diagram  
图 13 精跟踪模块光路图



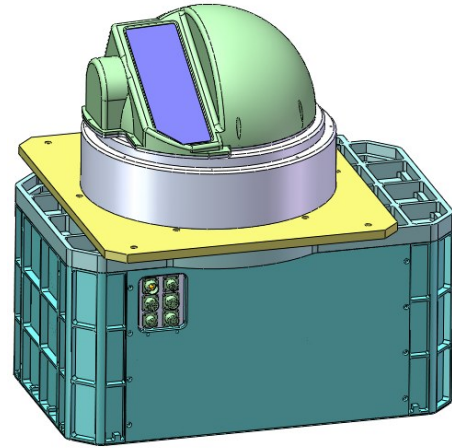
(a)



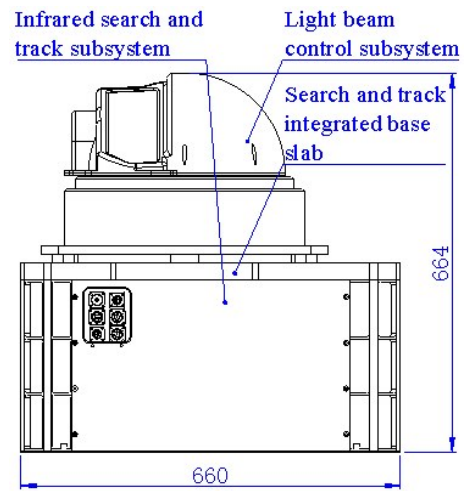
(b)

Fig. 14 Fine track module MTF: (a) 33 lp/mm MTF; (b) 17 lp/mm MTF  
图 14 精跟踪模块 MTF: (a) 33 线对/mm MTF; (b) 17 线对/mm MTF

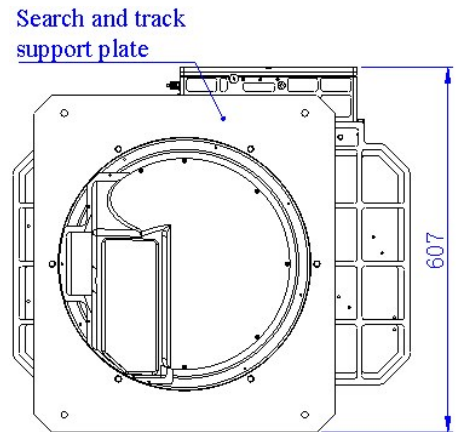
as the system installation structure. The size of the ADMWIRSTS is 660 mm (length) × 607 mm (width) × 664 mm (height), and the weight of the ADMWIRSTS is less than 68 kg. The system aperture is 80 mm.



(a)



(b)



(c)

Fig. 15 Integrated design of ADMWIRSTS: (a) 3D model; (b) front view; (c) upper view  
图 15 主动探测中波红外搜跟踪系统集成设计: (a) 三维模型; (b) 前视图; (c) 上视图

The ADMWIRSTS is taken as a whole model, and the finite element simulation analysis of the internal optomechanical structure is carried out. After simplifying the structure and adding mechanical coordination to the model, material parameters are added to the parts, and fixed

constraints are added to the search and track support plate installation surface. In the actual use environment, the gravity load is added to the model, and the influence of vibration is considered. The acceleration load of  $24.5 \text{ m/s}^2$  is applied to the whole machine in the direction of gravity by increasing 1.5 times of gravitational acceleration.

After meshing, the stress and displacement simulation analysis is carried out, as shown in Fig. 16. The maximum stress of the active detection system structure is at the reinforcement of the lens support structure of the search and coarse track module. The maximum stress is 0.98 MPa. The maximum stress of the structure is small, which will not affect the use of the system. It can be seen that the structural strength is sufficient. The maximum displacement of the system is in the front of the lens structure of the search and coarse track module. The maximum displacement is  $2.67 \times 10^{-3} \text{ mm}$ , and the displacement is small. It can be seen that the structural displacement will not affect the system performance, and the system design is reasonable and reliable.

#### 4.2 Infrared search and track imaging verification

After the actual processing, assembly and integration of the ADMWIRSTS designed in this paper, the out-field infrared imaging of the distant urban building exterior is carried out in front of the floor-to-ceiling window on the roof. The imaging results are shown in Fig. 17. Figure 17(b) is a panoramic search imaging image obtained by stitching the continuous imaging images of the search and coarse track module when the pitch scanning mirror of the light beam control subsystem rotates in the azimuth direction. Figure 17(c) is the coarse track staring imaging image of the search and coarse track module in the track mode. Figure 17(d) is the fine track staring imaging image of the fine track module in the track mode.

The main function of the fine track module in the system is to accurately identify and locate the echo of the illuminating laser based on the "cat-eye effect". In the design of the optical system, the energy of the fine track module is mainly concentrated in the working wavelength band of the illuminating laser, the energy collected from the external scene by the fine track module is weak, and the image contrast needs to be increased when imaging important objects.

Since the focal length of the fine track module is 4 times that of the search and coarse track module, the resolution of the fine track image of Fig. 17(d) is higher than that of the coarse track image of Fig. 17(c). For the same target, the fine track module obtains more detailed information of the building and improves the resolution accuracy of the system. As can be seen from Fig. 17, the search and coarse track module, and the fine track module have clear image quality and good imaging in the system's infrared search and track imaging.

#### 4.3 Experimental verification of active-detection technology

The active detection technology of the ADMWIRSTS is experimentally verified in the laboratory, as shown in

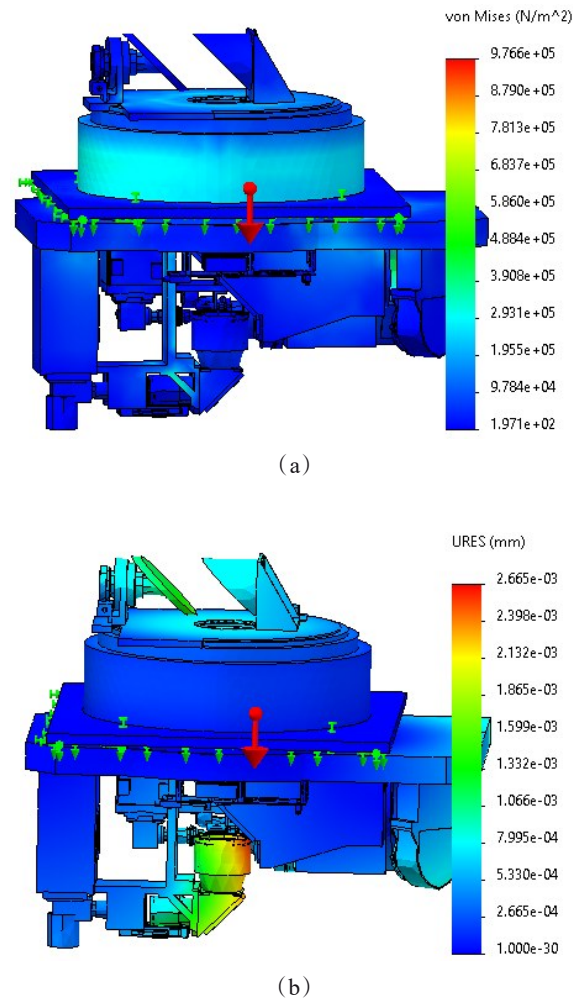


Fig. 16 Structure finite element analysis of ADMWIRSTS: (a) structural stress; (b) structural displacement  
图 16 主动探测中波红外搜跟系统结构有限元分析: (a) 结构应力; (b) 结构位移

Fig. 18. The active detection system is installed in front of the parallel light tube in the laboratory. After the infrared imaging of the large circular hole target and the small circular hole target in front of the thermostatic blackbody of the parallel light tube, the illumination laser is emitted to verify the active detection technology based on the "cat-eye effect". As shown in Fig. 18(b), the search and coarse track module emits an illumination laser after imaging the large circular hole target. The laser converges to a bright spot on the large circular hole target through the convergence of the parallel light tube. The clear imaging of the illumination laser can be obtained by the fine track imaging shown in Fig. 18(c). In Fig. 18(d), the search and coarse track module emits an illumination laser after imaging the small circular hole target. The laser converges to a bright spot on the left side of the small circular hole target. The clear imaging of the illumination laser can be obtained by the fine track imaging shown in Fig. 18(e). In Fig. 18(d), the target recognition locking in infrared search and track is turned on,

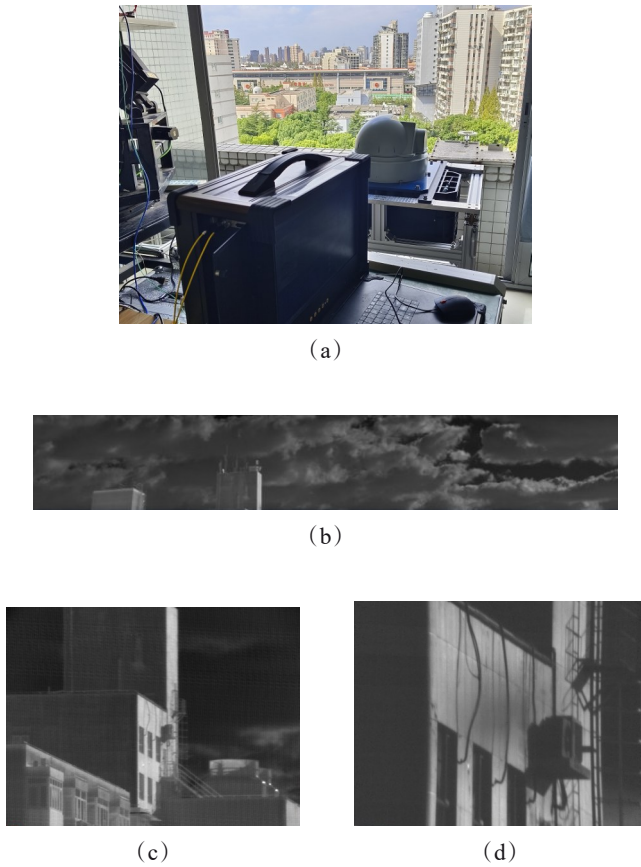


Fig. 17 Outfield imaging of infrared search and track: (a) out-field imaging; (b) panoramic search imaging diagram; (c) coarse track imaging diagram; (d) fine track imaging diagram  
图 17 红外搜跟外场成像: (a)外场成像; (b)全景搜索成像图; (c)粗跟踪成像图; (d)精跟踪成像图

and the small circular hole target and the illumination laser are locked.

In the optical design, the fine track module mainly receives energy in the working band of the illumination laser. Without image contrast enhancement, Fig. 18(c) and Fig. 18(e) only image the converging illumination laser, which can verify the fine track module's ability to accurately identify and locate the optical lens of the mid-wave imaging system. In Fig. 18(c), the illumination laser is imaged on the blackbody and deviates from the imaging focal plane of the parallel light tube, so the imaging is more divergent. In the corresponding Fig. 18(e), the illumination laser is imaged on the target, and the laser convergence position is closer to the imaging focal plane, and the imaging is more concentrated. Figure 18(c) and Fig. 18(e) have some diffuse reflections around the image due to the rough surface of the imaging position.

As can be seen from Fig. 18, the ADMWIRSTS based on "cat-eye effect" can actively detect and accurately identify and locate the infrared guidance or infrared detection system through the illumination echo of the illumination laser in the infrared search and track imaging. The engineering use effect is good.

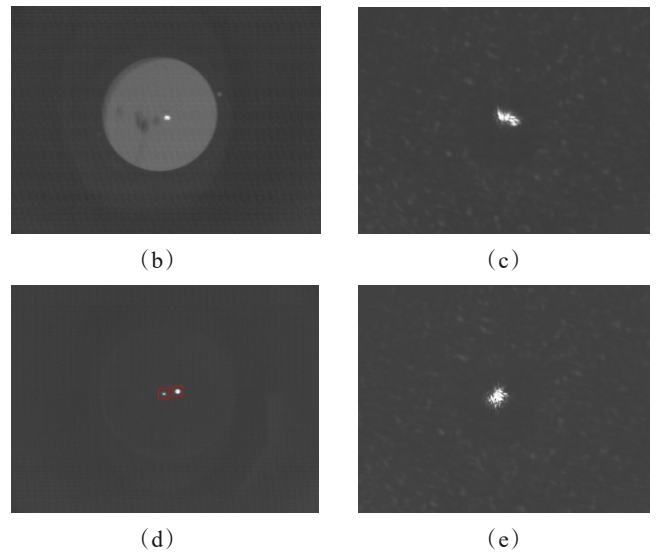
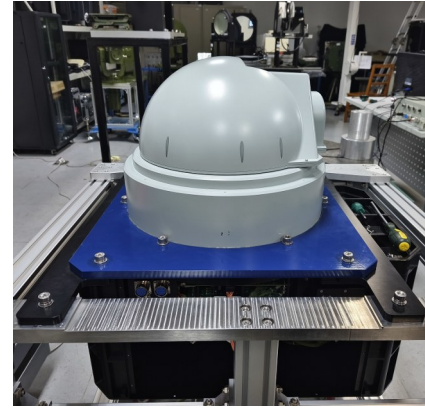


Fig. 18 Experimental verification of active detection technology: (a) laboratory imaging; (b) search and coarse track large target illumination imaging; (c) fine track large target illumination imaging; (d) search and coarse track small target illumination imaging; (e) fine track small target illumination imaging  
图 18 主动探测技术实验验证: (a)实验室成像; (b)搜索及粗跟踪大目标照明成像; (c)精跟踪大目标照明成像; (d)搜索及粗跟踪小目标照明成像; (e)精跟踪小目标照明成像

## 5 Conclusions

In this work, a set of active-detection mid-wave infrared search and track system (ADMWIRSTS) based on "cat-eye effect" was developed. The system includes a light beam control subsystem using an opto-mechanical integrated miniaturized two-dimensional pointing mechanism and an infrared search and track subsystem with infrared search, two-stage track, and illumination laser common aperture emission. The size of the system is 660 mm (length)  $\times$  607 mm (width)  $\times$  664 mm (height), and the weight of the system is less than 68 kg. The system structure meets the requirements of compact and lightweight engineering.

The co-aperture transmission and reception design of infrared search and track and illumination laser is carried out in the active detection system. The single pixel

instantaneous field of view of the search and coarse track module is 0.136 mrad, and the single pixel instantaneous field of view of the fine track module is 34.1  $\mu$ rad. Through the integration of light beam control and infrared search and track, the ADMWIRSTS realizes the search and track imaging of mid-wave infrared, and the accurate identification and positioning of active detection of infrared guidance or infrared detection system. The system completes the application integration of infrared search, infrared track and light beam control functions through integrated opto-mechanical design, and finally realizes the integrated application of infrared search and track, and illumination laser. The ADMWIRSTS developed in this paper is currently working in the mid-wave infrared band, and has certain target infrared spectrum recognition limitations. In the future, the ADMWIRSTS will develop in the direction of spectral recognition expansion, extending the working band to short-wave infrared and long-wave infrared, and the reserved high-energy laser interface will integrate infrared high-energy laser to make the ADMWIRSTS have the ability of laser suppression.

With the continuous improvement of the infrared recognition ability of moving targets, the research results of this paper can be applied to the new infrared guided moving target protection system. Through the active detection, accurate identification and positioning function in infrared search and track imaging, the target is locked in the two-stage aiming of coarse track and fine track. The reserved high-energy laser interface can emit high-energy laser to deal with the threat of high infrared recognition ability of moving targets. The research results have important academic and technical significance and practical application value for the development of compactly-integrated high-precision infrared search and track, and laser suppression system to meet the wider needs of security, anti-terrorism and so on, and have broad application prospects in the protection of important targets.

## References

- [1] ZHOU Yu Ping, WANG Jian Ying. Countermeasures against IR guided missile by airplane and its trend [J]. *Infrared and Laser Engineering*, 2006, 35(S1): 183-187.
- [2] ZHANG Qi. Application and research of infrared imaging guidance technology [D]. Beijing: Beijing Institute of Technology, 2015.
- [3] SUN Ming Wei. The demand for precision strike ammunition guidance technology in the 21<sup>st</sup> century [J]. *AERODYNAMIC MISSILE JOURNAL*, 2006, (02): 49-59.
- [4] LIANG Wei, ZHANG Ke. Development and Key Technologies of Precision-guidance Weapon [J]. *Fire Control & Command Control*, 2008, 33(12): 5-7, 12.
- [5] LIU Fei, SHAO Xiao-Peng, HAN Ping-Li, et al. Detection of infrared stealth aircraft through their multispectral signatures [J]. *Optical Engineering*, 2014, 53(9): 094101.
- [6] GREALISH K, KACIR T, BACKER B, et al. An advanced infrared thermal imaging module for military and commercial applications [C]. *Proc. of SPIE*, 2005, 5796: 186-192.
- [7] De Maarten V, Piet B W, Johannes F, et al. Passive ranging using an infrared search and track sensor [J]. *Optical Engineering*, 2006, 45(2): 1-14.
- [8] Boyd D S, Petitcolin F. Remote sensing of the terrestrial environment using middle infrared radiation (3.0 - 5.0  $\mu$ m) [J]. *International Journal of Remote Sensing*, 2004, 25(17): 3343-3368.
- [9] Crépy B, Clossé G, Cussat-Blanc S, et al. MILDA: mid-infrared laser source for DIRCM application [C]. *Proc. of SPIE*, 2013: 85430D.
- [10] LIU Zhong Ling, YU Zhen Hong, LI Li Ren, et al. Status and Development Trend of Infrared Search and Track System [J]. *MODERN DEFENCE TECHNOLOGY*, 2014, 42(02): 95-101.
- [11] ZHAO He Peng, DANG Ling. Development Prospect of Ship Infrared Search and Tracking System [J]. *OPTICS & OPTOELECTRONIC TECHNOLOGY*, 2022, 20(05): 129-134.
- [12] ZHU Yun. Review of New Generation Shipborne Staring Infrared Search and Tracking System Abroad [J]. *Ship Electronic Engineering*, 2023, 43(05): 19-25.
- [13] SHI Yong Shan, ZHANG Zun Wei. Development of Infrared Search and Track System [J]. *ELECTRO-OPTIC TECHNOLOGY APPLICATION*, 2016, 31(04): 11-14, 72.
- [14] LECOCQ C, DESHORS G, LADO-BORDOWSKY O, et al. Sight Laser Detection Modeling [C]. *Proc. of SPIE*, 2003, 5086: 280-286.
- [15] LIN Y B, ZHANG G X, LI Z. An improved cat's-eye retroreflector used in a laser tracking interferometer system [J]. *Meas. Sci. Technol.*, 2003, 14(6): 36-40.
- [16] He Ting, Niu Yan Xiong, Zhang Peng, et al. Original analysis and influence of the focal shift on the retro-reflected power of cat's eye effect [J]. *Infrared and Laser Engineering*, 2012, 41(11): 2956-2960.
- [17] MIEREMET A L, SCHLEIJPEN R M A, POCHELLE P N. Modeling the detection of optical sights using retro-reflection [C]. *Proc. of SPIE*, 2008, 6950: 45-49.
- [18] Zhao Yan Zhong, Sun Hua Yan, Song Feng Hua, et al. Research on the mechanism of reflection characteristics of laser irradiation on cat eye optical lens [J]. *ACTA PHYSICA SINICA*, 2008, 57(4): 2284-2294.
- [19] Qing Guang Bi, Wang Xue Kai, Guo Yong, et al. Physical model of "cat eye effect" and its certification [J]. *LASER TECHNOLOGY*, 1995, 19(04): 244-248.
- [20] SHI Jia Ming, WANG Feng. Review of foreign army optoelectronic countermeasure equipment [J]. *CONMILIT*, 2005, (10): 40-42.
- [21] ZHAO Peng Hao. Design and implementation of anti-photoelectric detection system based on "cat-eye effect" [D]. Yangzhou: Yangzhou University, 2020.
- [22] ZHAO Xun Jie, GAO Zhi Yun, ZHANG Ying Yuan. Technique of active laser reconnaissance and the applications in the military [J]. *OPTICAL TECHNOLOGY*, 2003, 29(4): 415-417.